

On a conversion of airborne MSS data into reflectance by using a simulation model

M.Shikada, K.Miyakita and Y.Haba
Kanazawa Institute of Technology
7-1 Ogigaoka Nonoichimachi Ishikawa 921
Japan
Commission Number VII

ABSTRACT

There are some distortions in the remotely sensed imageries obtained by the airborne MSS. They are the angular effects caused mainly by the rough surface in the optical sense and other variables. The separation of the noise from signature is generally achieved by using the appropriate relationship between CCT data and ground surface reflectance measured exactly. The powerful reflection model, called the Equivalent Reflection Model, has been developed by us for the purpose of obtaining the precise rough surface reflectance. In this paper, the first order approximation formula is adopted for the relation between CCT data and simulated reflectance. As the result, we have been able to estimate noise coefficients of the formula mentioned above. We may conclude that the CCT data can be converted into the reflectance by using the first order approximation formula relating CCT data to ground surface reflectance simulated by the model.

1 Introduction

There are some advantages in the remotely sensed imageries obtained by the airborne MSS. Observable date, time, altitude and course can be chosen freely. The most advantageous point is that the observable data can be efficiently obtained in a wide area. Information of MSS data covers a wide field. However, in the present situation, most users who are applying the data for classification or other analysis do so in a limited manner.

In this paper, we describe how the equivalent reflectance in a paddy field can be estimated from airborne MSS data by using a simulation model. As is generally known, reflectance of the ground surface is altered by the solar zenith angle, viewing angle, observation time and observed conditions of the object due to its rough surface in an optical sense. We have developed a powerful reflection model, and called it the Equivalent Reflection Model. This model enables us to obtain the reflectance of a paddy field taking into consideration all conditions relating to the observation items. In this paper, the regression model was adopted for the relationship between CCT data and computed reflectance. As a result, we have been able to estimate the noises contained in the CCT data. Based on the results described above, we may conclude that the CCT data can be converted into the reflectance. CCT data which was temporally obtained by the airborne MSS may be analyzed in reflectance.

2 Characteristics of airborne MSS data and conversion method

2.1 Change of MSS data

The advantages of airborne MSS data are not always effectively analyzed. There are some distortions in the remotely sensed imageries obtained by the airborne MSS. These include the angular effects caused by the rough surface in the optical sense, atmospheric effects, system distortions and other variables. CCT data used for analysis inevitably contains the multiplicative noise in addition to other noises as well. It is also an important fact that the count levels of CCT data does not include the characteristics of reflectance on the ground surface.

2.2 Conversion method to reflectance and its problems

This theoretical method considers the separation of the noise from signature through the use of various parameters. These parameters are the transmittance of the atmosphere, solar constant, gain or offset coefficient for the conversion to CCT count level, and other variables. It is extremely difficult to obtain these parameters because a large number of these parameters are unknown or uncertain. In this study, an experimental method is adopted instead of a theoretical method. The experimental method considers the relationship between CCT data and ground surface reflectance, measured exactly and expressing the first order approximation formula. In this case, we observed the reflectance of a large target on the ground in the flight course. It is almost impossible to spread a large standard target every time in which reflectance is already known. The experimental method used to obtain reflectance on the ground has already been previously reported. Here, however, we will propose a simple method where by an object spread the target over a wide area on the ground surface can be used instead of a large standard target. The change of the reflection in the same object is the most difficult problem in this method, because the shadow ratio of rough surface varies with the measured direction or time. Therefore, when we observe the reflectance for the rough surface, the observation conditions must be considered.

2.3 Method of conversion to reflectance

Reflection models for the canopy (including the paddy field) have been reported elsewhere. W.A.Allen et al. applied the Kubelka Munk theory to the single layer canopy model in which the canopy is horizontally and vertically uniform. G.H.Suits et al. extended the single layer canopy model to the multi layer canopy model. Taking into account the effects caused by the sun lit and shaded soil, A.J.Richardson proposed the soil, plant and shadow model. There are, however, some important difficulties in their models for obtaining the simulated reflectance on the ground surface. Most notably their models can not explain the reflectance for the rough surface in examples such as a paddy field. Since 1981 the authors have been conducting the experiments to obtain the change of reflectance on a paddy field. As a result, we would like to propose a powerful new reflection model to offer some solutions to the above mentioned problems. This model allows us to obtain a series of the reflectance of the paddy field as

a function of the solar zenith angle and the viewing angles of the detector, provided that we know a set of parameters necessary to demonstrate the circumstances of the actual field. These circumstances include the reflection ratio of the leaves, the ground, and the height of the paddy and other variables. These parameters are not influenced by the observation direction or time. This model enables us to obtain the equivalent reflectance of the paddy field by considering the viewing angle, sun altitude and sun azimuth. Therefore, the first order approximation formula is adopted for the relationship between CCT data and computed equivalent reflectance. We have been able to estimate the multiplicative noise coefficient and additional noise constant contained in the formula. This coefficient and constant are exact parameters obtained only by equivalent reflectance which corresponds to CCT data.

3 Relationship between CCT data and Reflectance

3.1 Assumption of the first order approximation formula

CCT data contains many distortions. The problem in analyzing such CCT data lies in finding a way to uncouple the interaction of surface radiation from the combined radiation in order to determine the true values of each unknown parameter separately.

The symbols and their definitions used to assume the first order approximation formula are listed below.

$t_{xyk}(\lambda, \tau_k(\lambda))$	CCT data
$R_{xy}(\lambda)$	Reflectance on the ground surface
G	Multiplicative noise
C	Additional noise
x, y	Co-ordinate on the ground
λ	Spectral band
k	Flight No.
τ_k	Optical thickness of atmosphere to k and λ

The first order approximation formula, to obtain G and C , is given here.

$$t_{xyk}(\lambda, \tau_k(\lambda)) = G_k(\lambda, \tau_k(\lambda)) \cdot R_{xy}(\lambda) + C_k(\lambda, \tau_k(\lambda)) \text{ ----- (1)}$$

3.2 Problems for the measurement of the reflectance on the ground surface

Measurement methods used to obtain $R_{xy}(\lambda)$ in equation (1) defined in a previous section are not accurate. Because a man who is measuring an object alternately observes the ground surface and white standard target. In the case of airborne MSS, as the scan mirror rotates, it sequentially looks at the ground (90 FOV). If we conduct a measurement of ground surface in the same way as MSS, we have to consider the viewing angle, solar altitude and solar azimuth. However, it is almost impossible to simultaneously consider these conditions. In order to resolve these problems, it is necessary to carry out the measurements from a sufficiently high altitude to obtain a large view field. In the paddy field, for example, a 5 meter high platform is required to observe a sufficiently large area. Moreover, if we consider the sun azimuth or sun altitude, measurements ought to be conducted simultaneously with the MSS observation.

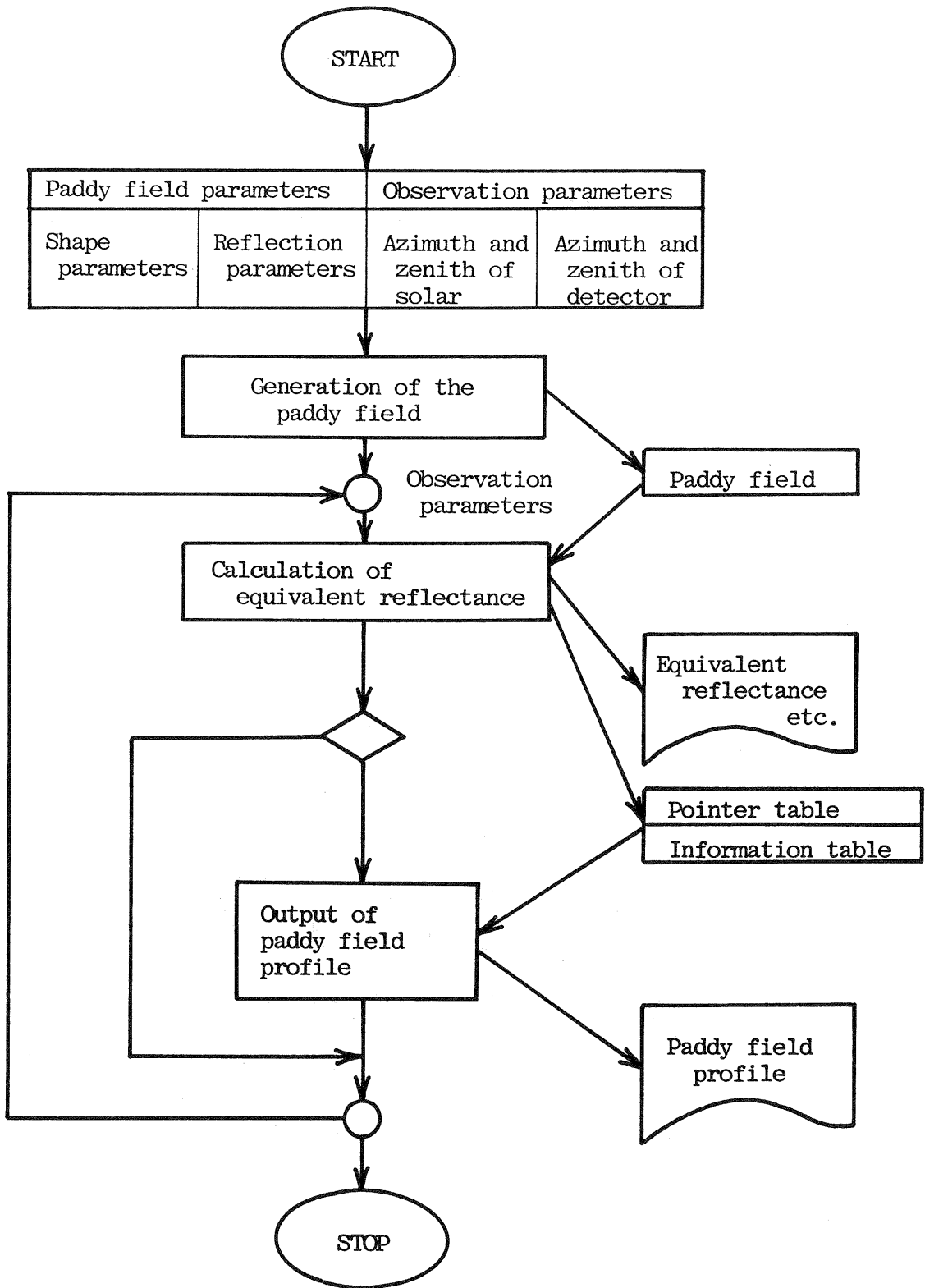


Fig.1 Flow diagram of software system

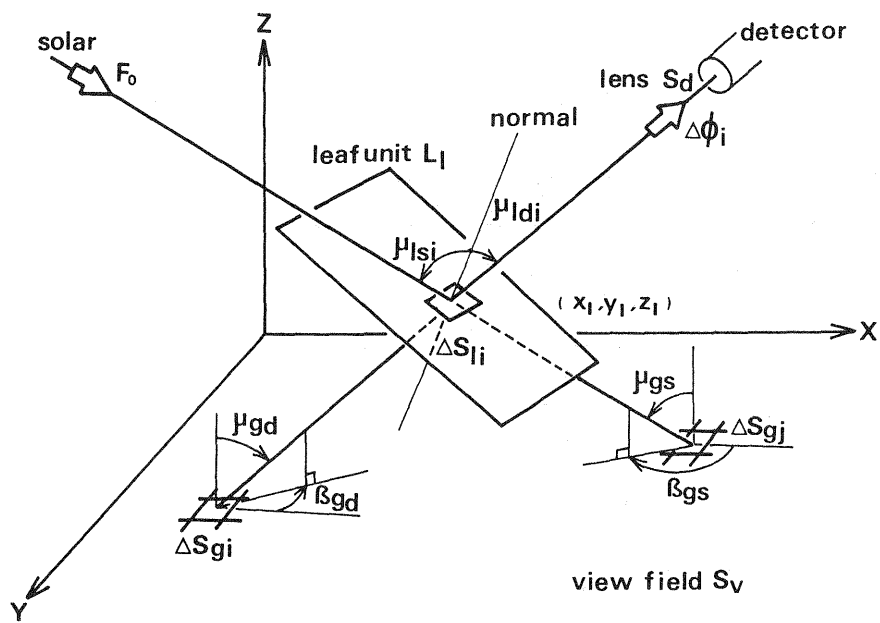


Fig.2 Illustration of observation system

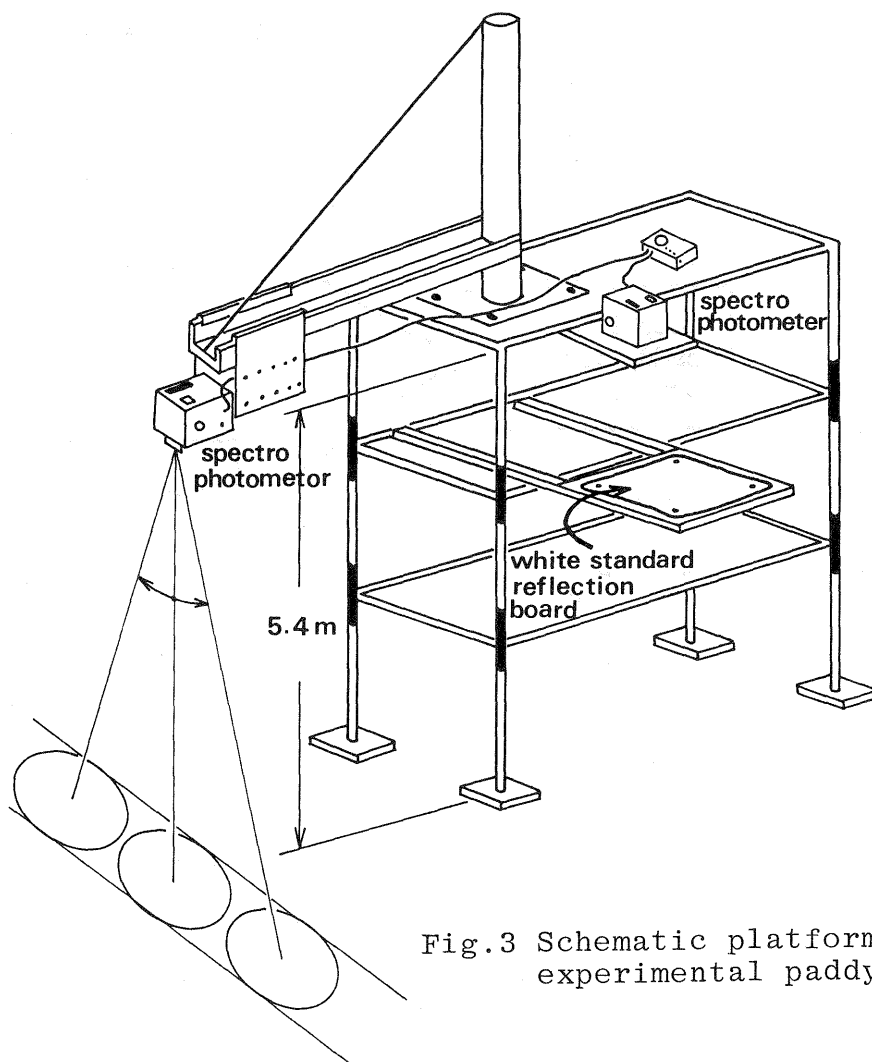


Fig.3 Schematic platform in the experimental paddy field

3.3 Conversion of CCT data

It is generally impossible to calculate theoretically the G_k and C_k defined by equation (1). We can estimate the multiplicative noise (G_k) and additional noise (C_k) by using ground surface reflectance (R_{xy}) and CCT data (t_{xyk}) at two points in the remotely sensed imageries. However, we have already found that the data measured from a low altitude and with a large view field angle does not almost coincide with the actual reflection data on the paddy field. We have been studying the variation of reflectance for the measurement conditions. As a result, we have developed a powerful reflection model, called the Equivalent Reflection Model, for the purpose of obtaining the precise rough surface reflectance taking into consideration the viewing angle, solar azimuth, solar zenith and other factors. This model enables us to eliminate complicated and tiresome observations. Equivalent reflectance of the paddy field is simulated by using this model. Multiplicative noise coefficient (G_k) and additional noise coefficient (C_k) can be estimated exactly from the relationship between the computed equivalent reflectance and CCT data. We have been conducting experimental research in order to convert the CCT data to ground surface reflectance by using these parameters.

4 Simulation model for the paddy field

4.1 Simulation model

A flow chart of the simulation model, called the Equivalent Reflectance Model, is shown in Fig.1. The advantage of this model is that we can easily create various situations of a paddy field by manipulating parameters such as leaf length, width, numbers, inclination angle of leaf units and other conditions. As a first step, this program begins with the input from these parameters. The flexibility in establishing these parameters is its most noticeable characteristic. The second step of this program simulates the false paddy field by using the parameters mentioned above. The next step of this program computes the equivalent reflectance. We assumed that the sun shines on the paddy field of this model and casts shadows on leaves, on the ground and/or on the leaves themselves. Moreover, we assumed that the detector casts shadows on the ground and/or on other leaves just as the sun does. The aspect for these are shown in Fig.2. By means of checking the types of shadows on the ground and determining the area of the shadows, we can easily obtain the equivalent reflectance. The last step of this program prints out the computed result and input parameters.

4.2 Verification of simulation model

We conducted a field measurement to compare simulation results with field data. It is desirable that ground truth observation is carried out from a sufficiently high altitude to maintain accuracy. Thus a platform was constructed in the experimental field by using iron pipes easily obtained. The

two spectro photometers were attached to the top of a 5 meter high platform to observe both the paddy field and white standard reflection board simultaneously. A schematic diagram of the platform is shown in Fig.3. We illustrate both the field measurement and simulation results on 22 of June 1982 and 23 of June 1983 in Fig.4 and Fig.5. The wavelength of these measurements and simulations were 650nm. The horizontal axis and vertical axis in Fig.4 show the viewing angle of the detector in degree and reflection ratios. In Fig.5, the viewing angle and equivalent reflectance are shown. It is important to remember that the reflectance of the paddy field is affected by the viewing angle and measured time. Similar characteristics can be found in both the field measurement results and computed ones. These results suggest that the equivalent reflectance of the paddy field can be estimated exactly by the simulation model.

4.3 Application of simulation to MSS data

The observation conditions of MSS which were applied to the simulation are shown in Table 1. The parameters which were used in the calculation of the equivalent reflectance were adopted from the data measured between 1982 and 1986. In our calculation, the average value of these parameters was used from the actual. Moreover these parameters were selected from the data measured within a week. The results of the simulation of viewing angle, wavelength and observation time are presented in Table 2. The curves in Fig.6, Fig.7 and Fig.8 show the change of equivalent reflectance on Table 2. The horizontal axis and vertical axis in these figures show the viewing angle of the detector in degree and simulated equivalent reflectance respectively. These results indicate that the reflectance is altered by the observation conditions.

5 Discussion

5.1 Change of CCT data with viewing angle

The MSS data shown in Table 1 was observed by observing a 10-20 km length area in our local region. Field of vision and flight conditions were quite good. Signals from the scanner were monitored and controlled in flight at the operator console and were recorded in analog form by a wideband magnetic tape recorder. The recorded signals were usually digitized and reformatted at a later time on the ground. CCT data had 803 pixels in one line. The airborne MSS data used in this study was collected by a JSCAN-AT-12M MSS system with 11 channels. The airborne MSS spectral bands for data processing are shown in Table 3. The wavelengths which were simulated by the model were 450nm, 550nm and 650nm. For this reason, band3, band5 and band7 were used in this study. Almost all training area were covered by paddy fields. It is generally considered that the maximum frequency of row pixel's CCT data is nearly equal to the radiation from the paddy field. Table 4 shows the maximum frequency of row pixel's CCT data at intervals of 10 degree per viewing angle. 0 degree represents the center of the scanning angle. CCT data was collected from a scanning center to +- 40 degrees at intervals of 10 degrees. Data presented () in

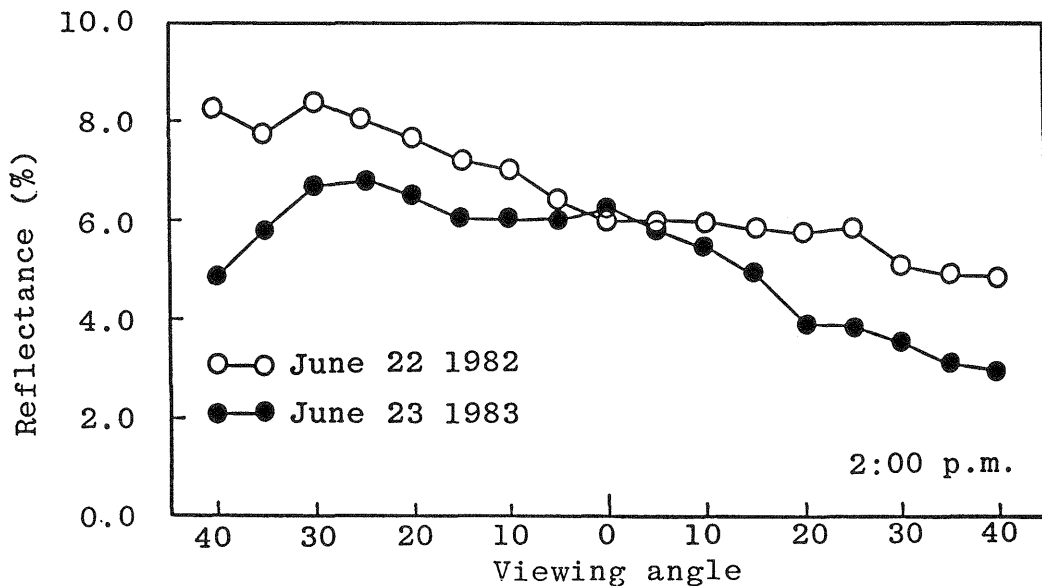
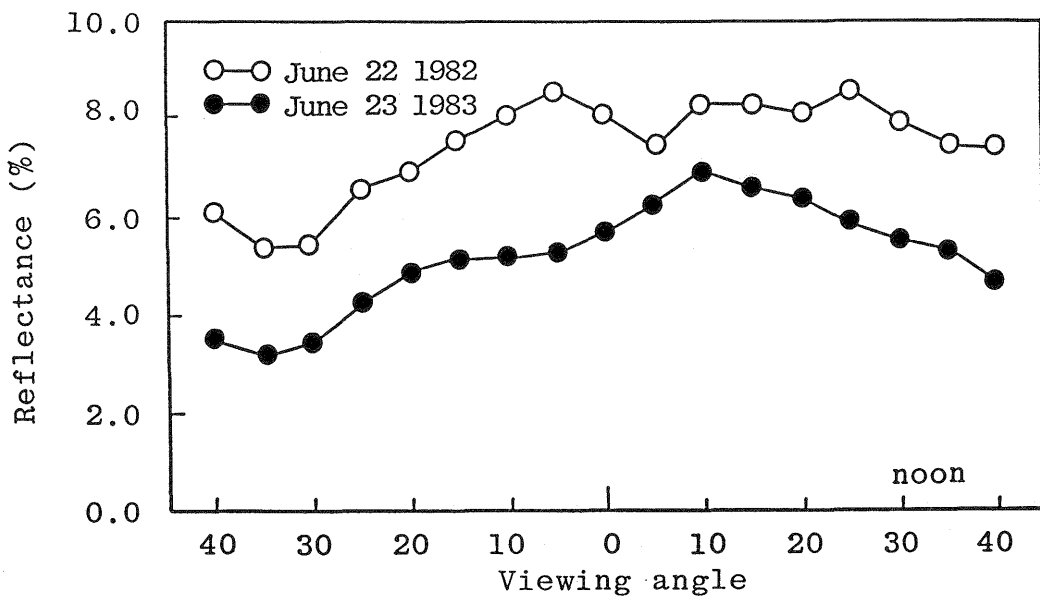
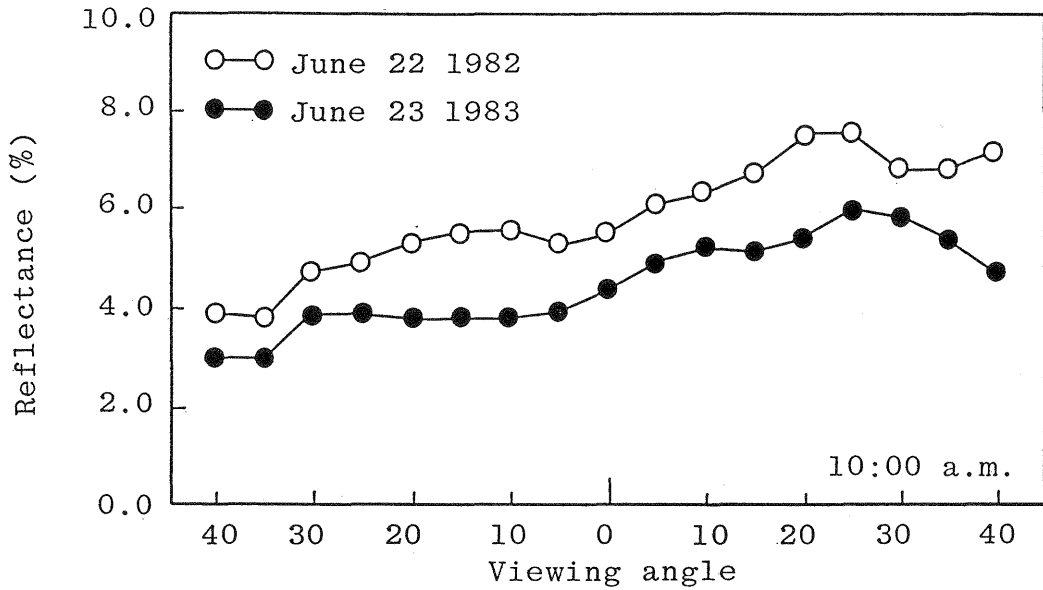


Fig.4 Reflectance relating to viewing angle for observation time (Observed reflectance of the experimental paddy field)

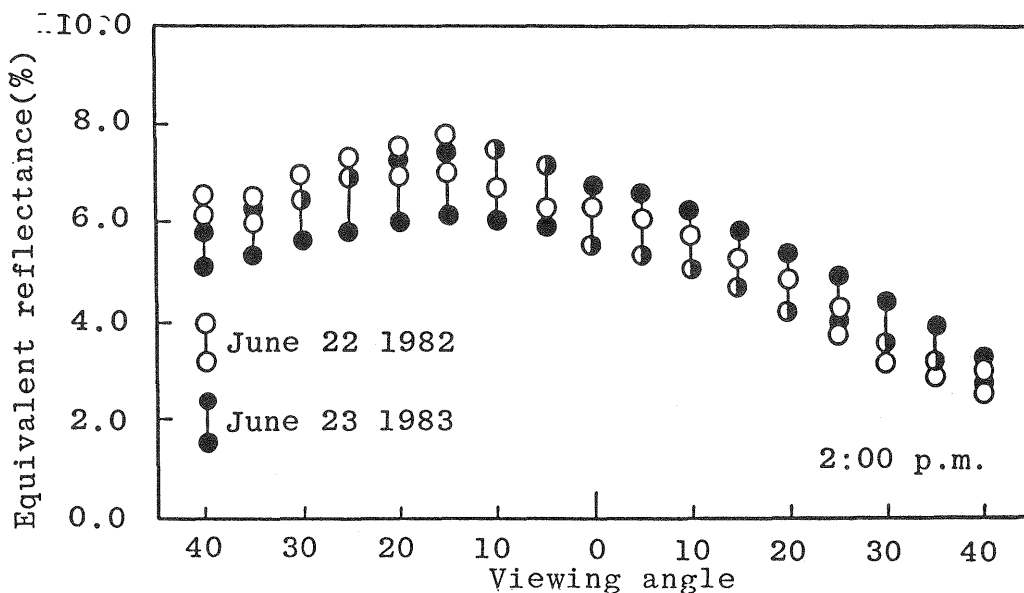
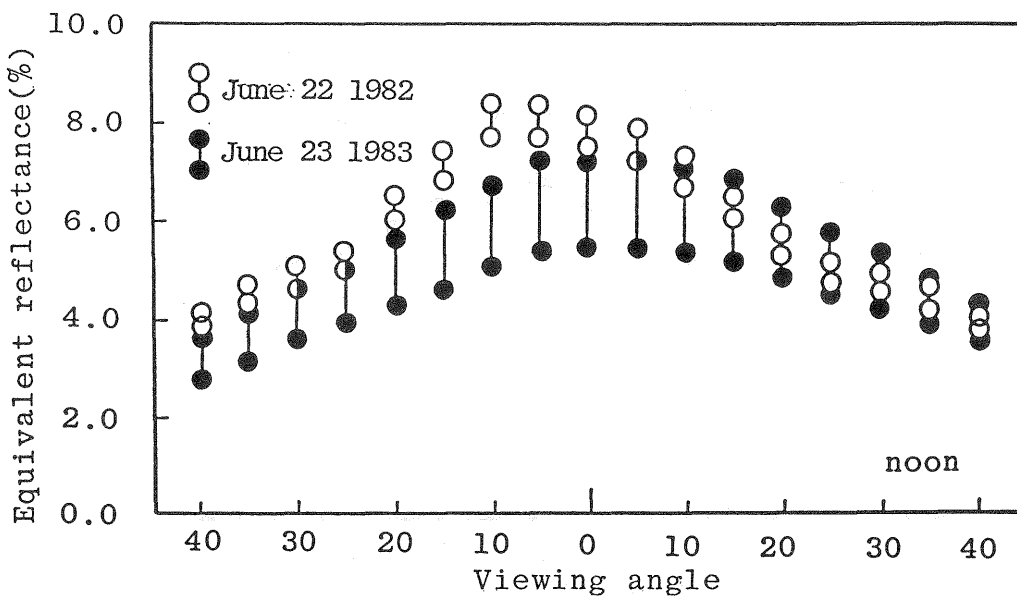
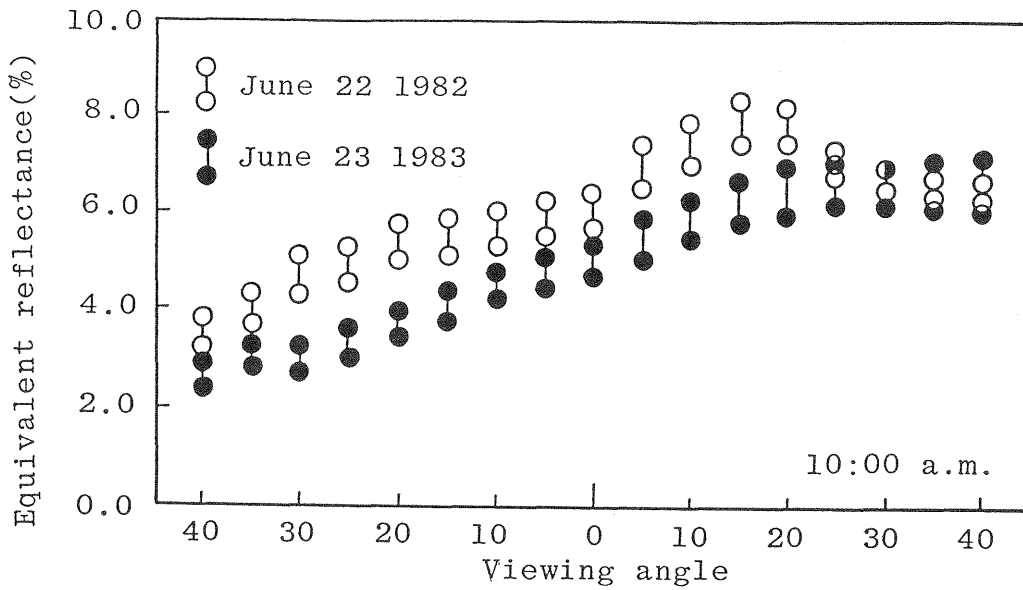


Fig.5 Reflectance relating to viewing angle for observation time (Equivalent reflectance obtained by computer simulation)

Table 1 Memorandum Concerning MSS Observation

Flight No.	Flight Date	Flight Time	Flight Altitude	flight Direction	Solar Azimuth	Solar Zenith	Observed Area
1	1978.7.30	11:09	3,700ft	SSW 30°	S 40 E	22.2	KANAZAWA-TURUGI
2	1978.7.30	12:01	11,200ft	SSW 30°	S	15.6	KANAZAWA
3	1979.8.31	15:29	10,200ft	NNE 20°	S 74 W	55.6	KANAZAWA

Table 2 Equivalent Reflectance Obtained by Computer Simulation

Simulation No.	Simulation Date, Time	Wavelength (nm)	Viewing Angle								
			40	30	20	10	0	10	20	30	40
1	30 July	450	2.69	2.46	2.22	2.06	2.28	2.68	2.82	2.98	3.04
	1978	550	7.20	6.72	6.19	5.90	6.64	7.89	8.37	8.96	9.17
	11:00	650	2.52	2.58	2.66	3.09	3.98	4.98	5.27	5.53	5.57
2	30 July	450	1.63	1.73	1.92	2.29	3.27	3.60	3.66	3.75	3.64
	1978	550	5.99	5.94	6.10	6.61	10.04	9.84	10.18	10.63	10.43
	12:00	650	3.02	3.15	3.45	4.03	5.85	6.33	6.49	6.70	6.52
3	31 Aug.	450	2.29	2.10	1.87	1.52	1.23	1.08	1.05	1.01	0.99
	1979	550	6.98	6.52	6.05	5.35	5.28	5.86	5.71	6.13	6.37
	15:30	650	3.38	3.29	3.07	3.02	2.35	1.96	1.93	1.96	2.05

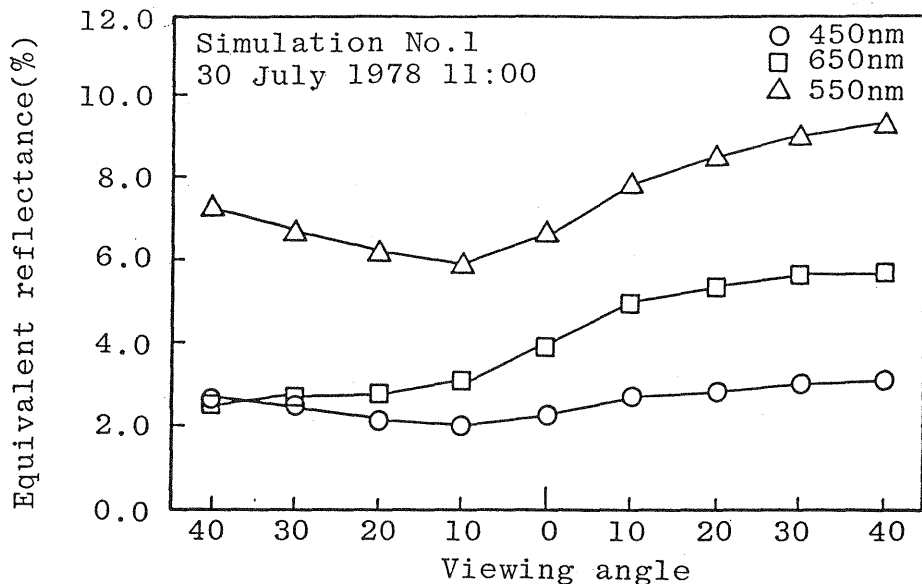


Fig.6 Change of equivalent reflectance for viewing angle

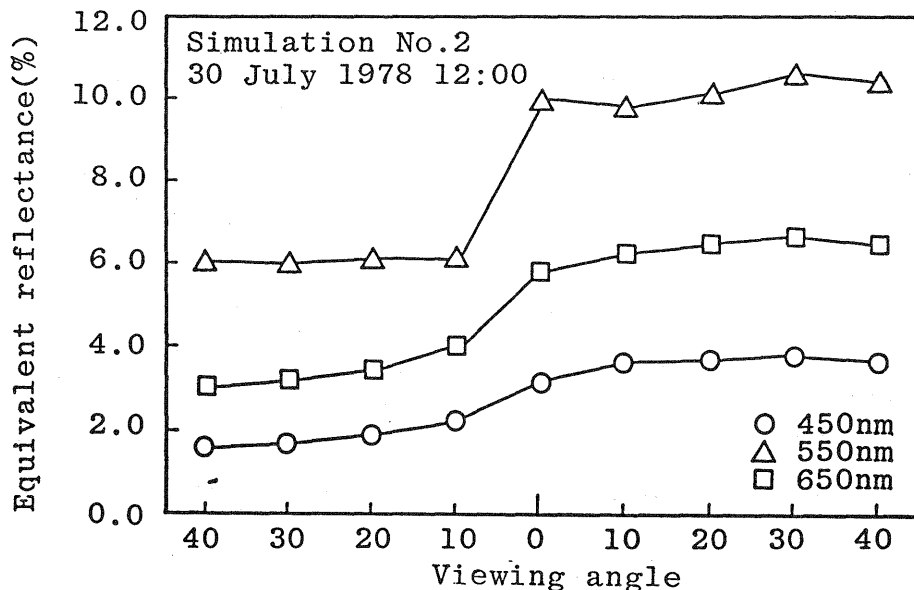


Fig.7 Change of equivalent reflectance for viewing angle

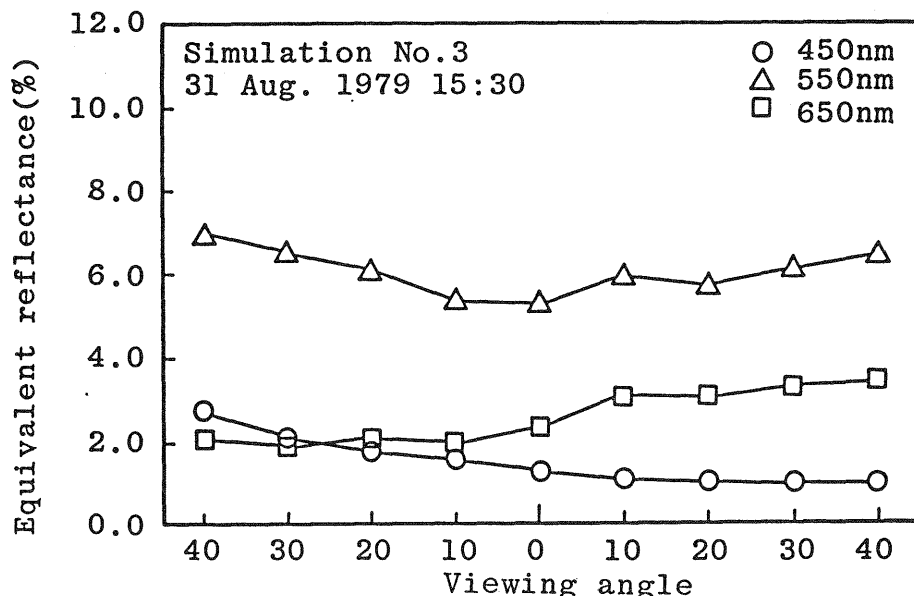


Fig.8 Change of equivalent reflectance for viewing angle

Table 3 Spectral Band of Airborne MSS (JSCAN-AT-12M)

Channel No.	Wavelength(μm)	Channel No.	Wavelength(μm)
0	0.25 - 0.35	6	0.60 - 0.65
1	0.35 - 0.40	7	0.65 - 0.70
2	0.40 - 0.45	8	0.70 - 0.80
3	0.45 - 0.50	9	0.80 - 0.90
4	0.50 - 0.55	10	0.90 - 1.10
5	0.55 - 0.60	11	8.00 -14.00

Table 4 Change of CCT Data for Viewing angle

Flight No.	Flight Date,Time	Band	Viewing Angle								
			40	30	20	10	0	10	20	30	40
1	30 July 1978	3	(39)	(39)	43	43	47	51	54	51	51
	11:00	5	(59)	(53)	60	62	67	79	84	87	78
		7	(59)	(57)	65	66	69	77	80	77	77
2	30 July 1978	3	39	39	46	51	53	(53)	(51)	(51)	(51)
	12:00	5	47	48	66	71	82	(77)	(75)	(72)	(73)
		7	40	43	50	59	63	(64)	(59)	(59)	(59)
3	31 Aug. 1979	3	124	110	100	95	94	(93)	(77)	(80)	(84)
	15:30	5	107	98	89	83	84	(84)	(51)	(51)	(54)
		7	82	75	71	66	65	(67)	(43)	(43)	(43)

Table 4 contains the radiation levels from various objects including the paddy field ,because the all observation area is not the paddy field itself. The diagrams in Fig.9 ,10 and Fig.11 illustrate the data in Table 4. The horizontal axis and vertical axis in these figures show the viewing angle of the detector in degree and maximum frequency of CCT count respectively. The plots represented by coloring black in the graph refer to the radiation from various objects including the paddy field, that correspond to the data presented () in Table 4.

5.2 Estimation of G_k and C_k

If the relationship between CCT data and equivalent reflectance simulated by the model is represented by equation(1), we can estimate the multiplicative noise coefficient G_k and additional noise constant C_k contained in equation (1). It is necessary to determine the equivalent reflectance and CCT data for more than two points respectively. The data shown in Table 5 represents the G_k and C_k calculated by the least square method using the data in Table 2 and Table 4. But we did not use the data presented () in Table 4 in this operation.

5.3 Evaluation of G_k and C_k

Thus, based on the results represented in Table 5, we can conclude that the multiplicative noise coefficient G_k and additional noise constant C_k changes with wavelength. If we apply these coefficient to equation(1), then the CCT data can be converted into ground surface reflectance. This model enables us to evaluate the CCT data which was observed at different time period in the reflectance. The results of converted reflectance from CCT data are presented in Table 6.

6 Conclusion

In this study,the conversion of CCT data into reflectance by a simulation model was examined.

The summary of the results is as follows;

(1) CCT data used for analysis inevitably contains the noise and is necessary to exclude from CCT data for conversion into reflectance.

(2) The noise was separated into multiplicative noise and additional one. Equation(1) was determined by the relationship between the CCT data and ground surface reflectance.

(3) To obtain a converted reflectance from the CCT data in equation(1),the exact reflectance on the ground surface was necessary. We developed a powerful reflection model to obtain a series of the reflectance of a paddy field as a function of a measurement system. We conclude that the computed reflectance by the model agrees with the reflectance values actually obtained from in field measurement. As a results,we were able to estimate the multiplicative noise coefficient and additional

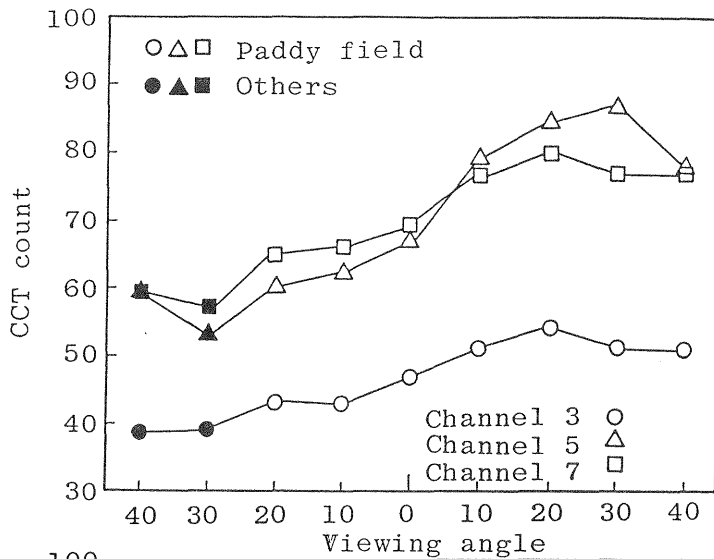


Fig.9 Change of CCT data for viewing angle (maximum frequency of row pixel's data)

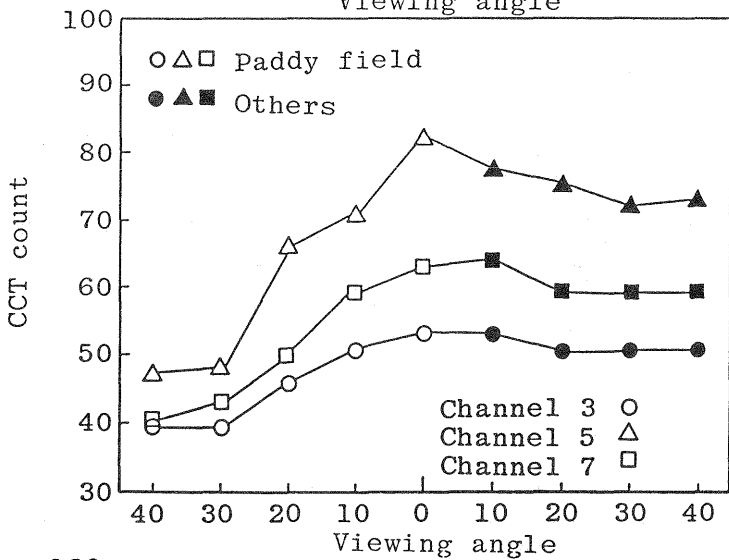


Fig.10 Change of CCT data for viewing angle (maximum frequency of row pixel's data)

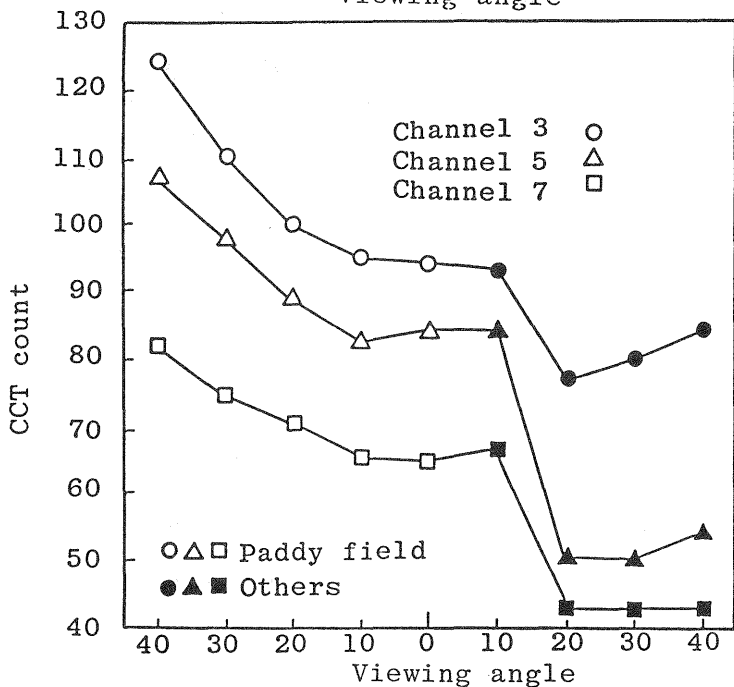


Fig.11 Change of CCT data for viewing angle (maximum frequency of row pixel's data)

Table 5 G_{λ} and C_{λ} Calculated by Least Square Method

Flight No.	Flight Date	Flight Time	G_{λ}			C_{λ}		
			G_3	G_5	G_7	C_3	C_5	C_7
1	30 July	11:09	11.2	0.45	4.94	-19.6	-17.5	-50.8
2	30 July	12:01	8.68	6.63	7.34	-26.8	-16.7	-22.0
3	30 Aug.	15:29	20.0	12.2	16.6	-69.0	-18.4	-21.3

Table 6 Comparison between Equivalent Reflectance and Converted Reflectance from CCT data

Flight No.	Flight Date, Time	Wavelength	Viewing Angle								
			40	30	20	10	0	10	20	30	40
1	30 July 11:00 1978	Model 450nm	(2.69)	(2.46)	2.22	2.06	2.28	2.68	2.82	2.98	3.04
		CCT3→Ref.	(1.73)	(1.73)	2.09	2.09	2.45	2.80	3.07	2.80	2.80
		Model 550nm	(7.20)	(6.72)	6.19	5.90	6.64	7.89	8.32	8.96	9.17
		CCT5→Ref.	(5.57)	(4.77)	5.70	5.97	6.64	8.26	8.93	9.33	8.12
		Model 650nm	(2.52)	(2.58)	2.66	3.09	3.98	4.98	5.27	5.53	5.57
		CCT7→Ref.	(1.66)	(1.25)	2.87	3.08	3.68	5.30	5.91	5.30	5.30
2	30 July 12:00 1978	Model 450nm	1.63	1.73	1.92	2.29	3.27	(3.60)	(3.66)	(3.75)	(3.64)
		CCT3→Ref.	1.40	1.40	2.21	2.79	3.02	(3.02)	(2.79)	(2.79)	(2.79)
		Model 550nm	5.99	5.94	6.10	6.61	10.0	(9.84)	(10.2)	(10.6)	(10.4)
		CCT5→Ref.	4.57	4.72	7.44	8.19	9.85	(9.10)	(8.79)	(8.34)	(8.49)
		Model 650nm	3.02	3.15	3.45	4.03	5.85	(6.33)	(6.49)	(6.70)	(6.52)
		CCT7→Ref.	2.45	2.86	3.81	5.04	5.59	(5.75)	(5.04)	(5.04)	(5.04)
3	31 Aug. 15:30 1979	Model 450nm	2.29	2.10	1.87	1.52	1.23	(1.08)	(1.05)	(1.01)	(0.99)
		CCT3→Ref.	2.75	2.05	1.55	1.30	1.25	(1.20)	(0.40)	(0.55)	(0.75)
		Model 550nm	6.98	6.52	6.05	5.35	5.28	(5.86)	(5.71)	(6.13)	(6.37)
		CCT5→Ref.	7.26	6.52	5.79	5.29	5.37	(5.37)	(2.67)	(2.67)	(2.92)
		Model 650nm	3.38	3.29	3.07	3.02	2.35	(1.96)	(1.93)	(1.96)	(2.05)
		CCT7→Ref.	3.66	3.23	2.99	2.69	2.63	(2.75)	(1.31)	(1.31)	(1.31)

noise constant by analyzing the relationship between computed reflectance and the CCT data.

(4) We applied this coefficient and constant to equation(1). Then the CCT data was converted into the ground surface reflectance. The converted reflectance from the CCT data coincides good agreement with the computed reflectance by the model.

(5) The model developed has the advantage that the parameters for simulation in field measurement can easily be obtained.

This research was supported by Matto High School of Agriculture. We wish to acknowledge Mr. Shibata and his workers for their generosity, especially, in allowing us the use of their paddy field. We also thank those K.I.T. students who assisted in the collecting of the data and helped in the computer simulation.

REFERENCES

W.A.Allen and A.J.Richardson; Interaction of Light with a Plant Canopy, *J.Opt.Soc.America*, 53-8, 1023/1028 (1968)

G.H.Suits; The calculation of the Directional Reflectance of a Vegetative Canopy, *Remote Sensing of Environment* 2, 117/125 (1972)

A.J.Richardson, et al.; Plant, Soil, and Shadow Reflectance Component of Row Crops, *Photogrammetric Engineering and Remote Sensing*, 41-11, 1401/1407 (1975)

J.H.Colwell; Vegetation Canopy Reflectance, *Remote Sensing of Environment* 3, 175/183 (1974)

Y.Haba, M.Shikada and K.Miyakita; On a New Reflection Model for the Corn Field, *The Sixteenth International Symposium on Remote Sensing of Environment*, 893/903 (1982)

M.Shikada, K.Miyakita and Y.Haba; A Study on the Estimation of Equivalent Reflectance in the Paddy Field by the Simulation Model, *JSPRS*, Vol.26, 43/52, (1987)

K.J.Ranson et al.; Sun-View Angle Effect on Reflectance Factors of Corn Canopies, *Remote Sensing of Environment* 18, 147/161 (1985)

M.Shibayama, C.L.Wiegand; View Azimuth and Zenith, and Solar Angle Effects on Wheat Canopy Reflectance, *Remote Sensing of Environment* 18, 91/103 (1985)